

See discussions, stats, and author profiles for this publication at: <https://www.researchgate.net/publication/239390640>

# Wind-Field and Filling Models for Hurricane Wind-Speed Predictions

ARTICLE *in* JOURNAL OF STRUCTURAL ENGINEERING · NOVEMBER 1995

Impact Factor: 1.5 · DOI: 10.1061/(ASCE)0733-9445(1995)121:11(1700)

---

CITATIONS

79

---

READS

154

2 AUTHORS, INCLUDING:



Peter J Vickery

Applied Research Associates, Inc.

46 PUBLICATIONS 1,551 CITATIONS

SEE PROFILE

# WIND-FIELD AND FILLING MODELS FOR HURRICANE WIND-SPEED PREDICTIONS

By Peter J. Vickery<sup>1</sup> and Lawrence A. Twisdale,<sup>2</sup> Members, ASCE

**ABSTRACT:** Two key modeling components in the hurricane simulation process are the wind-field model, and the filling model, which describes the rate of decay of the hurricane after landfall is made. In the investigation described here, new wind-field and filling-rate models are developed for use in hurricane simulation routines. Detailed evaluations of the wind-field and filling models used in 1980 by Batts et al., which are used to develop the hurricane wind speeds given in ASCE-7-88, and the new wind-field and filling models are performed. Results indicate that the combination of wind-field and filling models employed in the original study used to derive hurricane wind speeds given in ASCE-7-88 yield significant overestimates of hurricane wind speeds at inland locations, and their wind-field model is unable to reproduce the high surface-level wind speeds evident in very intense storms. The deficiencies in the models used by Batts et al. are carried through to the recommended design wind speeds given in ASCE-7-88.

## INTRODUCTION

This paper describes a new wind-field model and new filling-rate models developed for use in hurricane simulations. The new wind-field model described here incorporates the most recent information on hurricane gust factors, and the model is validated through comparisons to over 20 full-scale records of hurricane wind speeds. The wind-field model is based on the numerical model described in Shapiro (1983). New hurricane filling models are developed for three different regions of the United States. The new filling models reproduce the observations that more intense storms fill more rapidly than weak storms. The filling-rate models are evaluated with results of detailed filling-rate studies performed by Ho et al. (1987). The wind-field and filling-rate models used by Batts et al. (1980) are also evaluated through comparisons to full-scale data. The wind-field and filling models used by Batts et al. (1980) are examined because the results obtained from their study form the basis for the design wind speeds given in ASCE-7-88 ("Minimum" 1990). Results indicate that the filling-rate model used by Batts et al. (1980) produces simulated storms that decay much too slowly when compared to actual decay rates, and the Batts wind-field model overestimates wind speeds away from the coast and underestimates wind speeds within the eye wall of hurricanes at the coast.

## WIND-FIELD MODELS

### Shapiro-Based Wind-Field Model

The wind-field model described here employs the numerical solution of the equations of motion of a hurricane developed by Shapiro (1983). The numerical model developed by Shapiro (1983) is very similar to that originally developed by Chow (1971); however, Shapiro (1983) used a truncated spectral analysis to diagnose the boundary-layer flow field instead of solving the full nonlinear model as was done in Chow (1971). The original work of Shapiro (1983) was directed towards examining the effect of surface friction on the asymmetries in hurricane windfields. Georgiou (1985) also used the Shapiro wind-field model in his investigation of hur-

ricane winds along the Gulf and Atlantic Coasts of the United States; however, the implementation of the Shapiro model in this study differs from that used by Georgiou. In Shapiro (1983), the momentum equations for a slab boundary layer of constant depth under an imposed symmetric pressure distribution are solved. The coordinate system moves with the hurricane vortex, which is in gradient balance with the pressure field above the boundary layer. The radial and tangential momentum equations in cylindrical coordinates ( $r, \lambda$ ) are

$$u \frac{\partial u}{\partial r} - \frac{v^2}{r} - fv + \frac{v}{r} \frac{\partial u}{\partial \lambda} + \frac{\partial \phi}{\partial r} - K \left( \nabla^2 u - \frac{u}{r^2} - \frac{2}{r^2} \frac{\partial v}{\partial \lambda} \right) + F(c, u) = 0 \quad (1a)$$

$$u \left( \frac{\partial v}{\partial r} + \frac{v}{r} \right) + fu + \frac{v}{r} \frac{\partial v}{\partial \lambda} - K \left( \nabla^2 v - \frac{v}{r^2} + \frac{2}{r^2} \frac{\partial u}{\partial \lambda} \right) + F(c, v) = 0 \quad (1b)$$

where  $u$  and  $v$  = vertically integrated average values of the radial and tangential components of the velocity;  $\phi$  = pressure distribution within the storm;  $c$  = translation speed of the hurricane;  $f$  = Coriolis parameter;  $K$  = a constant coefficient of eddy diffusion;  $r$  = radial distance from the storm center;  $\lambda$  = angle measured counterclockwise from an easterly direction; and  $F$  = frictional drag force. The frictional drag force acts parallel to the total velocity vector and is given as

$$F(c, u) = (C_D/h)|\mathbf{u} + \mathbf{c}|(\mathbf{u} + \mathbf{c}) \quad (2)$$

where  $\mathbf{u}$  and  $\mathbf{c}$  = vector components of the circulation-induced wind speed and the storm translation speed, respectively; and  $h$  = boundary-layer depth assumed to be a constant value of 1 km over the domain of the storm. The drag coefficient,  $C_D$ , used by Shapiro (1983) is based on the model developed by Deacon (Roll 1965) and varies linearly with velocity in the following form:

$$C_D = (1.1 + 0.04|\mathbf{u} + \mathbf{c}|) \times 10^{-3} \quad (3)$$

The drag coefficient expressed in (3) was originally developed for surface-level winds (10 m above the sea surface); consequently, for consistency, when used with upper-level (or vertically averaged) winds,  $C_D$  should be reduced by the ratio  $(V_{10}/V_u)^2$  where  $V_u$  = value of the vertically integrated wind speed and  $V_{10}$  = wind speed 10 m above the water surface, suggesting that  $C_D$  should be reduced to between 50% and 70% of the 10-m value. In this study, a value of  $C_D$  reduced to 50% of that given in (3) is used. The modeling of the sea-surface drag coefficient as linearly dependent on wind

<sup>1</sup>Sr. Engr., Applied Research Associates, Inc., Raleigh, NC 27615.

<sup>2</sup>Prin. Engr., Applied Research Associates, Inc., Raleigh, NC.

Note. Associate Editor: Ahsan Kareem. Discussion open until April 1, 1996. Separate discussions should be submitted for the individual papers in this symposium. To extend the closing date one month, a written request must be filed with the ASCE Manager of Journals. The manuscript for this paper was submitted for review and possible publication on December 3, 1993. This paper is part of the *Journal of Structural Engineering*, Vol. 121, No. 11, November, 1995. ©ASCE, ISSN 0733-9445/95/0011-1700-1709/\$2.00 + \$.25 per page. Paper No. 7458.

speed is considered by some researchers [e.g., Amoroch and Devries (1980) and Donelan (1982)] to be too simplistic. These researchers suggest a drag-coefficient model should recognize the existence of breaking waves. The results of Amoroch and Devries (1980) indicate that for mean wind speeds (at 10 m above sea level) greater than 20 m/s, a full breaker saturation state exists and the drag coefficient (based on the 10-m wind speed) is constant and equal to 0.0254, in which case modeling the geostrophic drag coefficient as a constant in the range of 0.02–0.03 would be more appropriate. The studies by Donelan (1982) indicate that the drag coefficient may be influenced by the direction of the waves with respect to the mean wind, with waves traveling in a direction opposite that of the wind yielding the higher values of  $C_D$ , resulting in a drag coefficient varying over the domain of the storm. The effect of varying the surface drag coefficient on the windfield is discussed in more detail in Twisdale and Vickery (1992).

The pressure distribution of  $\phi = \phi_0(r)$  is assumed to be symmetric and in gradient balance with a specified vortex with a gradient wind  $v_{gb}(r)$  so that

$$\frac{\partial \phi}{\partial r} = \frac{v_{gb}^2}{r} + f v_{gr} \quad (4)$$

The vortex is defined with a 30-km wide cubic spline transition region connecting a solid body rotation in the inner core in the form  $(r/R_{max})$ , to a profile in the form of  $(r/R_{max})^{-n}$  in the outer vortex.  $R_{max}$  is the radial distance from the center of the storm to the location where the maximum wind speeds occur. In Shapiro (1983), the profile exponent,  $n$ , is assigned a value of 0.62; however, we examined other values of  $n$  in this investigation. Shapiro (1983) solves the momentum equations with the relative wind decomposed into a spectral representation where

$$u = u_0(r) + u_{c1}(r)\cos \lambda + u_{s1}(r)\sin \lambda + u_{c2}(r)\cos 2\lambda + u_{s2}(r)\sin 2\lambda \quad (5a)$$

$$v = v_0(r) + v_{c1}(r)\cos \lambda + v_{s1}(r)\sin \lambda + v_{c2}(r)\cos 2\lambda + v_{s2}(r)\sin 2\lambda \quad (5b)$$

where the subscripts  $c$  and  $s$  refer to the sine and cosine portions of the expansion.

The grid spacing used to solve (1) is variable, with a uniform grid of  $\Delta r = 5$  km for  $r < 2R_{max}$ . For  $r > 2R_{max}$ , the grid spacing increases linearly out to a radius of 1,300 km. The output from the Shapiro model consists of 91 coefficients of each  $u_0, u_{c1}, u_{s1}$ , etc. Solving the momentum equations in spectral form does not produce a solution as accurate as the full nonlinear solution; but, because the entire tropical cyclone windfield is represented with relatively few parameters, the technique has advantages for employment in Monte Carlo simulations, as discussed in Twisdale and Vickery (1992). To cover the full range and combinations of  $\Delta p$  (the difference in pressure between the center of the storm and the ambient pressure),  $R_{max}$ ,  $c$ , and  $f$  expected, we simulated 968 storms for each of a number of latitudes along the hurricane coastline of the United States. The coefficients generated for each storm are stored on disk and recalled as needed. Using the spectral modeling approach employed by Shapiro, 910 coefficients are read from disk for each storm. For each simulated storm the velocities  $u$  and  $v$  are found by interpolating from the  $\Delta p, R_{max}, c$ , and  $f$  results stored on disk.

The wind speeds produced by the numerical model are vertically averaged values defined as

$$V_u = \frac{1}{h} \int_0^h V(z) dz \quad (6)$$

where  $h$  = boundary-layer depth. The boundary-layer depth used by Shapiro (1983) and used here is 1 km. Assuming a neutral logarithmic boundary layer model in which

$$V(z) = V_h [\ln(z/z_0)/\ln(h/z_0)] \quad (7)$$

where  $V_h$  = wind speed at height  $h$ , yields values of  $V_u$  that are similar in magnitude to the wind speed of a height of 500 m for a wide range of roughness lengths  $z_0$ . For typical values of  $z_0$ , the difference between the vertically averaged wind speed and the wind speed at 500 m is about 2%. As a result, the vertically average wind speeds are taken as being equivalent to the upper-level wind speed at a height of about 500 m.

The upper-level winds are adjusted to surface level (10 m, over water) by applying a 17.5% reduction for  $r < 2R_{max}$  and a 25% reduction for  $R > 4R_{max}$ , with a smooth transition curve used for intermediate values of  $r$ . This reduction in wind speed to surface level (over water) is similar to that used in Georgiou (1985), where wind speed data given in Myers (1954) was used in his model development. The reduction in wind speed to the surface (with respect to upper-level wind speeds) is also consistent with the 0.8 rule as described and evaluated in Powell (1980).

As discussed in Shapiro (1983), the use of a vertically averaged boundary-layer model leads to excessive estimates of radial velocities (and thus inflow angles) compared to those obtained in a more sophisticated multilevel model. In this study it is assumed that the inflow angles computed using the reduced drag coefficient are consistent with those at the surface level, rather than upper-level values, thus compensating for the overestimate of the inflow angles associated with the use of a vertically averaged boundary-layer model.

No reference to an averaging time is given in Shapiro (1983); however, results are applicable to a long period (nonturbulent) average assumed to be about 1 h. During the model development and comparisons to full-scale data, other long-period averaging times were examined (e.g., 10 min, etc.). The assumption of a 1-h averaging time provided the best comparisons to full-scale data, and these comparisons are shown later.

The hourly surface-level wind speeds (i.e., wind speeds averaged over 1 h) are converted to fastest-mile values using the gust-factor curve developed by Krayner and Marshall (1992) specifically for hurricane winds. The estimated fastest-mile wind speeds are considered to be representative of hurricane winds at the coastline (i.e., over water wind speeds). To account for the effects of surface friction, these coastal surface-level winds are linearly decayed to standard exposure  $C$  conditions ( $V_s/V_u = 0.62$ ) over a distance of 30 to 50 km from the coastline (50 km for  $R < 2R_{max}$  and 30 km for  $R > 4R_{max}$ ), to enable estimates of wind speeds away from the coastline to be produced. The wind speed at a location  $x$  km from the coast,  $V_{sx}$  is given as

$$V_{sx}/V_u = (V_{sw}/V_u) - 0.004x; \quad V_{sx}/V_u \geq 0.62 \quad (8a,b)$$

where  $V_{sw}$  = surface wind speed at the coastline;  $V_u$  = upper-level, or vertically averaged, wind speed; and  $V_{sx}$  = surface wind speed  $x$  km from the coast. This linear reduction in wind speed with distance from the coast is more gradual than implied in some other investigations [e.g., Batts et al. (1980), Georgiou (1985), and Powell (1987)], however the comparisons between modeled and observed hurricane wind speeds tend to support the assumption for the case of onshore winds. This linear reduction in wind speed with distance from the coastline will lead to an overestimate of wind speeds near the coast when the wind is blowing from the land to the ocean (i.e., offshore winds). This overestimation of wind speeds for offshore winds is seen in comparisons of modeled and observed wind speeds for Hurricane Hugo, as discussed later.

## Batts Wind-Field Model

The wind-field model used by Batts et al. (1980) (referred to here as the Batts model) is a modification of the Standard Project Hurricane Windfield Model where the maximum gradient wind speed,  $V_{gx}$ , is given as

$$V_{gx} = K\sqrt{\Delta p} - (R_{\max}/2)f \quad (9)$$

where  $\Delta p$  = central pressure difference and  $K$  = a constant. The maximum 10-min wind speed at a height of 10 m over the ocean is given as

$$V(10, R_{\max}) = 0.865V_{gx} + 0.5c \quad (10)$$

where  $c$  = translation speed of the storm. The 10-min wind speed over the ocean at any point in the storm ( $r, \theta$ ) is

$$V(10, r, \theta) = V(10, R_{\max})V_r(r) - 0.5c(1 - \cos \theta) \quad (11)$$

where  $V_r(r)$  = ratio of the maximum 10-min wind speed at the radius of maximum winds to the 10-min mean at a distance  $r$  from the center of circulation. The ratio  $V_r(r)$  is given in Batts et al. (1980) in nomograph form. The angle  $\theta$  in (11) is measured from a line making an angle of  $115^\circ$  (clockwise) from the direction of motion of the storm so that the region of maximum winds (relative to the earth) is always in the right rear quadrant of the storm. The 10-min mean overland wind speed is obtained by multiplying the overwater wind speed by 0.85, implying an immediate reduction in wind speed at the ocean-coastline interface. No further reduction in wind speed produced by surface friction for locations further inland is allowed for. The 10-min mean wind speeds are converted to fastest mile values using the results of Durst (1960), which have been shown to be inappropriate in the case of hurricane winds (Kramer and Marshall 1992).

## Storm-by-Storm Comparisons

Because of the assumptions and empirical model components used in both the Shapiro-based wind-field model (e.g., drag coefficients, averaging time, inflow angles, etc.) and the Batts wind-field model, evaluation of the wind-field models through comparison to full-scale measurements is of critical importance, and provides the only means to evaluate the impact of the assumptions. Wind speeds estimated using both the Shapiro-based wind-field model and the Batts wind-field model were evaluated through comparisons to wind speeds measured in Hurricane Frederic (1979), Alicia (1983), Elena (1985), Hugo (1989), and Andrew (1992). In total, 26 detailed, full-scale wind-speed records were examined.

In all comparisons except Hurricane Andrew, information on  $\Delta p$ , storm position, direction, and translation speed used to evaluate the wind-field models was obtained from the 6-h position data given on the HURDAT diskettes. In the case of Hurricane Andrew, storm position and central pressure data were obtained from the National Hurricane Center (NHC) preliminary report on Hurricane Andrew. For Hurricane Hugo, additional information on  $\Delta p$  and position just before the time of landfall was obtained from Powell et al. (1991). A linear variation in central pressure with time was assumed between the known values. Radius to maximum wind data for each of the hurricanes were obtained from various sources. Given the information on  $\Delta p$ , storm position, and  $R_{\max}$  as a function of time for each storm, we simulated the hurricane winds at a particular site as a function of time by moving the mathematical models of the hurricane windfield along the path of the storm. The translation speed of the hurricane is determined from the position and time information. The simulated wind speeds determined at 15-min intervals were

adjusted to fastest mile values and compared to full-scale (measured) values.

In the case of Hurricane Alicia (1983), there is some controversy as to the value of  $R_{\max}$ . Ho et al. (1987), Golden (1984) and Willoughby (1990) suggest that near the time of the landfall,  $R_{\max}$  changed from about 28 km to near 58 km. Powell (1987) suggests that the apparent larger value of  $R_{\max}$  is associated with outer rain-band activity, rather than a change in  $R_{\max}$ . For the comparisons of simulated and observed wind speeds presented here, we found (using either wind-field model) that  $R_{\max}$  of 28 km best reproduced wind speeds at locations near the center of the hurricane track, but the larger value of  $R_{\max}$  reproduced wind speeds better at locations further removed from the center of the storm. Ho et al. (1987) indicated that the larger value of  $R_{\max}$  should be used for storm surge computations near Galveston. In the case of Hurricane Frederic, a constant value of  $R_{\max}$  of 35 km was used (Kaplan and Frank 1993; Powell 1982).  $R_{\max}$  for Hurricane Elena was set equal to 22 km (Willoughby 1990). For Hurricane Hugo,  $R_{\max}$  information was provided by Mark Powell of the National Oceanic and Atmospheric Administration/Hurricane Research Division (NOAA/HRD), and a constant value of 40 km was used in the simulations. For Hurricane Andrew in South Florida,  $R_{\max}$  was assigned a value of 18.5 km (Powell and Houston 1993).

Full-scale measurements of wind speed and direction for Hurricanes Alicia, Frederic, Elena, and Hugo, in the form of peak gust and/or 1-, 10-, 15-, or 30-min mean wind speeds, were provided by R. D. Marshall of the National Institute of Standards and Technology. Peak gust and/or mean wind-speed data were converted to fastest-mile equivalents using the gust-factor data given in Kraymer and Marshall (1992). Information on anemometer heights and the surface roughness,  $z_0$ , was provided by R. D. Marshall. In the case of Hurricane Hugo, additional information on anemometer height and roughness length was provided by P. R. Sparks of Clemson University. All wind speeds, except those near the coast, were converted to equivalent exposure C conditions ( $z_0 = 0.03$  m) using the procedure outlined in Marshall (1984). For coastal and offshore locations [U.S. Coast Guard Cutter (USCGC) Buttonwood for Hurricane Alicia, Data Buoy 42007 and Dauphin Island for Hurricane Elena, and the Molasses Reef and Fowey Rocks C-MAN stations for Hurricane Andrew] wind speeds are adjusted to the 10-m level using the local value of  $z_0$ , assumed to be 0.005 m. If the true value of  $z_0$  differs from the assumed value of 0.005 to between 0.001 and 0.02 m, and for anemometer heights in the range of 5–50 m, this assumption leads to maximum errors for mean wind speeds corrected to 10 m of less than  $\pm 4\%$ . In the case of the C-MAN stations when adjusting wind speeds to the 10-m level, no allowance for a change of the sea-surface roughness with wind speed is allowed for; however, the effective roughness length  $z_0$  varies relatively little over a relatively wide wind-speed range. For example, defining  $C_D$  using (3) and computing  $z_0$  from the following expression:

$$z_0 = 10 \exp(-k/\sqrt{C_{D10}}) \quad (12)$$

where  $k$  = von Karman constant ( $k = 0.4$ ) and is the drag coefficient based on the 10-m mean wind speed, leads to estimates of  $z_0$  ranging between 0.0024 and 0.0076 m for mean wind speeds at 10 m ranging between 30 and 50 m/s. These values of  $z_0$  support the assumed value of  $z_0$  equal to 0.005 for coastal locations, and the assumption results in little error when the wind speeds are converted to 10-m values.

Detailed comparisons of the observed and simulated wind speeds of 12 of the 26 records examined (6 near coastal and 6 inland locations) are given in Figs. 1 and 2. For all of the near-coast locations examined here, the simulated wind speeds

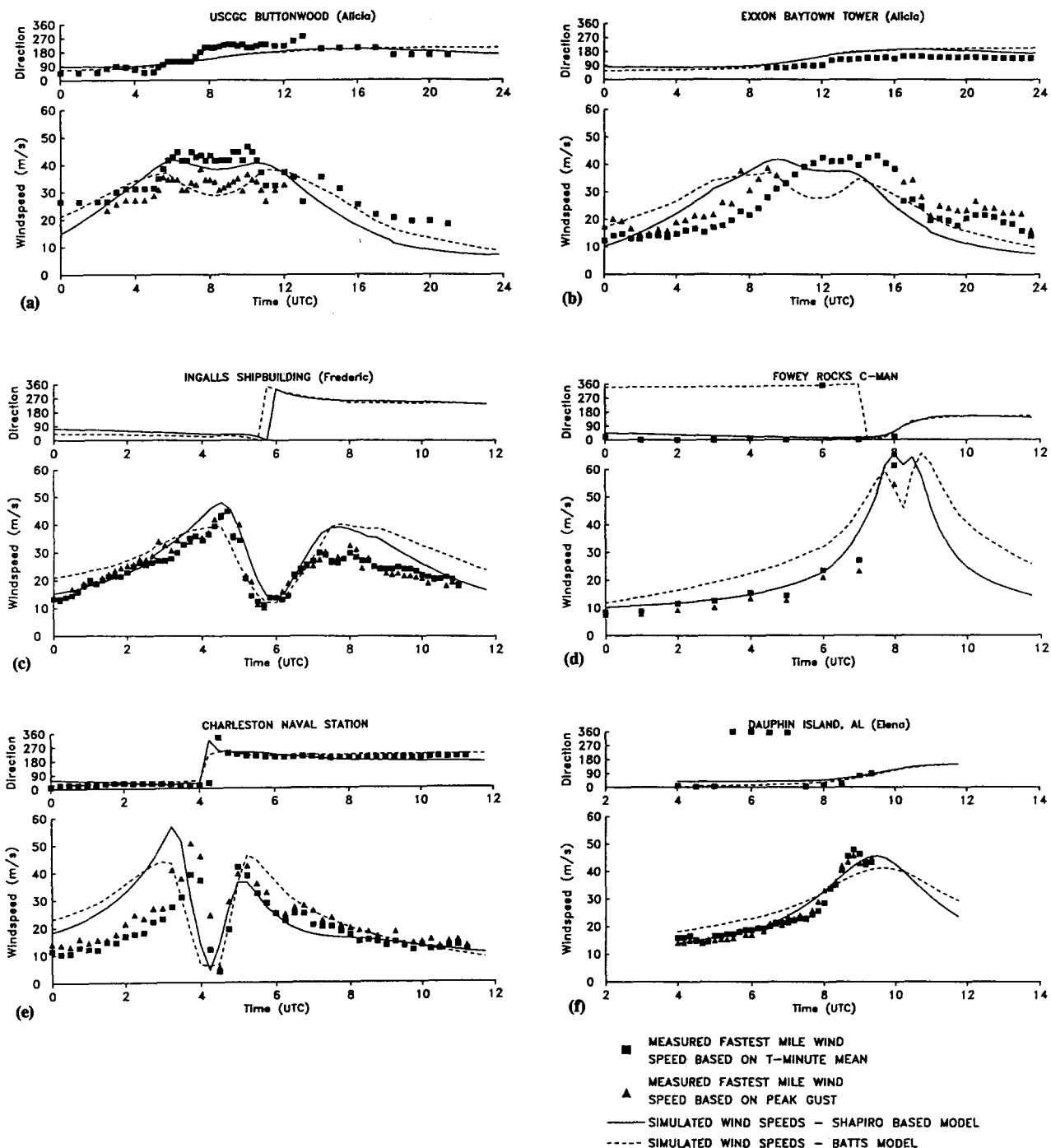


FIG. 1. Comparisons of Simulated and Observed Fastest-Mile Wind Speeds at Coastal Locations

derived using the Shapiro-based model are reduced as a linear function of the shortest distance to the coast. Fig. 1 shows comparisons of the Shapiro-based simulated fastest-mile wind speeds and measured fastest mile wind speeds obtained from the USCGC Buttonwood and the Exxon Baytown anemometer for Hurricane Alicia, Ingalls Shipyard for Hurricane Frederic, Dauphin Island for Hurricane Elena, Charleston Naval Base for Hurricane Hugo, and the Fowey Rocks C-MAN station for Hurricane Andrew. All of these stations are located within a few kilometers of the coast or just offshore, near the location of maximum winds. The comparison of the simulated and measured fastest-mile wind speeds at Dauphin Island, Ingalls Shipyard, and the USCGC Buttonwood all indicate that the Shapiro-based wind-field model provides a better representation of the measured wind speeds. At USCGC Buttonwood, the wind speeds obtained using the Shapiro-

based model agree well with the full-scale fastest-mile wind speeds derived from the 10-min averaged data, whereas the wind speeds predicted using the Batts model agree well with the lower fastest-mile wind-speed data derived from measured peak gusts. At Dauphin Island, the Batts wind-field model underpredicts the peak wind speeds by about 10%, whereas the Shapiro-based model underestimates the peak winds by about 2%. At Ingalls Shipyard, the Shapiro-based model overestimates the peak wind speeds by about 10%, whereas the Batts model again underestimates the peak winds by about 8%; both wind-field models overestimate wind speeds recorded after the passing of the eye of the storm, but this overestimation is greater with the Batts model. In the case of Charleston Naval Base (Hurricane Hugo), the fastest-mile wind speeds simulated using the Shapiro-based model before the passing of the eye are significantly higher than those de-

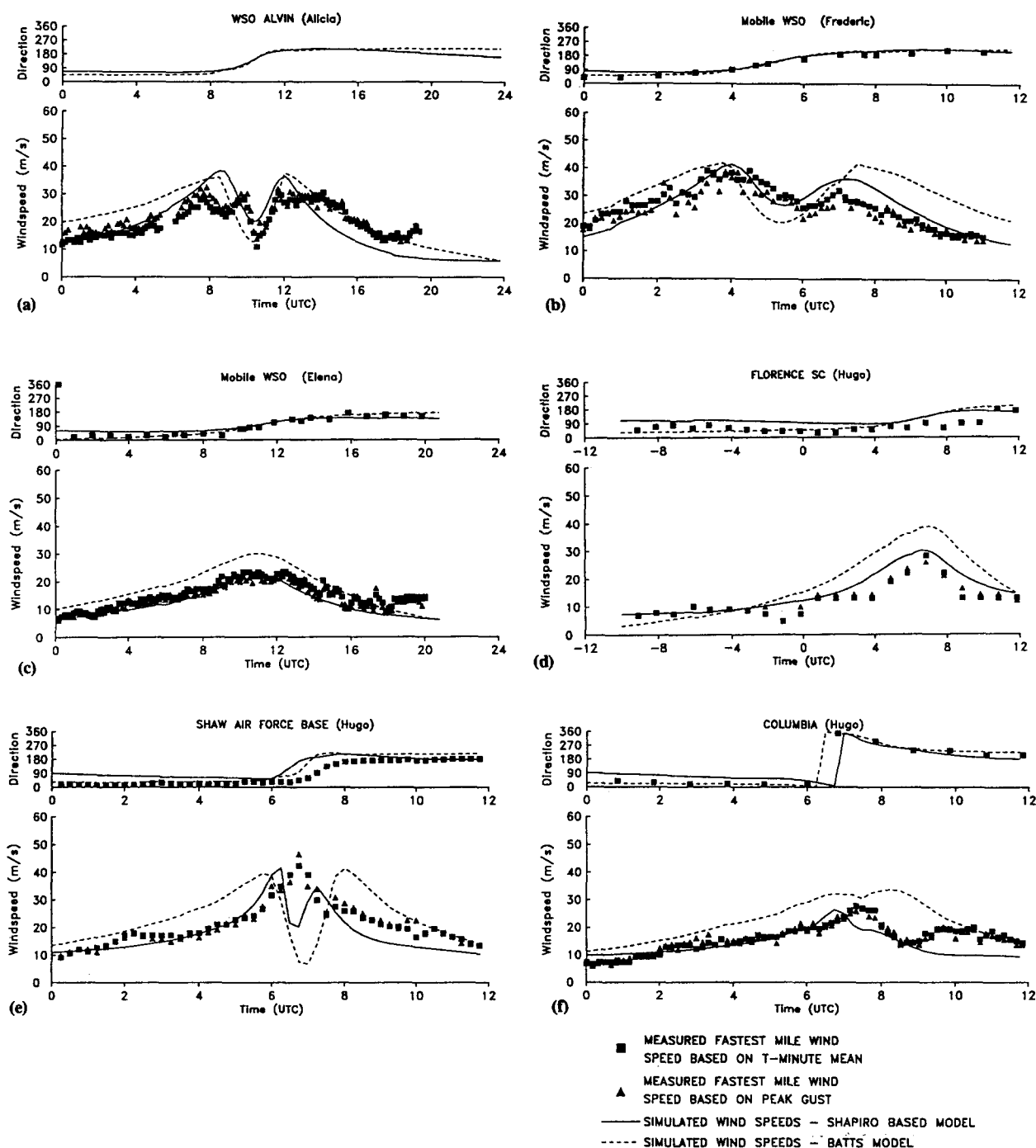


FIG. 2. Comparisons of Simulated and Observed Fastest-Mile Wind Speeds at Inland Stations

rived from either the measured peak gust or 10-min mean data, whereas after the passing of the eye the agreement is good. The peak wind speeds predicted by the Batts model before the passing of the eye wall agree well with the measured values, and slightly overestimate those occurring after the passing of the eye. At the two Charleston locations examined (Charleston Airport not shown), the Shapiro-based model overestimates the maximum wind speeds. This overestimation is thought to be a result of the winds approaching the anemometer sites having passed a much larger land fetch than at the other coastal locations examined (i.e., offshore winds in the Hugo case versus nearly onshore winds for other cases). This reduction in wind speed associated with frictional effects for the two Charleston locations is not treated in the implementation of the Shapiro-based wind-field model, where for an inland location, onshore winds are assumed (i.e., the wind speeds

are reduced as a linear function of the minimum distance to the coastline, without considering the fact that the wind may have blown over a longer land fetch if the station is located on the left hand side of a landfalling storm). No full-scale measurements of wind speed were obtained for Hurricane Hugo at locations experiencing the maximum onshore winds within the eye wall. Comparisons of the predicted and measured wind speeds recorded during Hurricane Andrew at the Fowey Rocks C-MAN station (located to the north of the track, on the right side of the storm, near the region of maximum winds) show the maximum fastest-mile wind speeds simulated using either model are approximately equal, but the shape of the wind-speed trace is better reproduced using the Shapiro-based model. Because the Fowey Rocks C-MAN station is located offshore, the 15% wind-speed reduction required for land-based stations is not used in the Batts model in this comparison.

Fig. 2 shows comparisons of simulated and measured wind speeds at six inland stations [the National Weather Service (NWS) Station at Alvin for Hurricane Alicia; Mobile, Ala., for Hurricanes Frederic and Elena; and Shaw Air Force Base, Florence Airport Station, and Columbia Airport for Hurricane Hugo]. The figure clearly indicates the Shapiro-based model best reproduces hurricane winds at inland locations. As discussed in Twisdale and Vickery (1992), further improvements in the comparison of observed and simulated wind speeds for inland stations can be obtained by adjusting the surface drag coefficient used in the numerical model to be consistent with local terrain conditions.

### Wind-Speed Prediction Error Analysis

Table 1 presents a summary of the percentage difference between the maximum measured and maximum simulated wind speeds obtained using the Shapiro-based model for 25 of the 26 records examined. The Fowey Rocks C-MAN measurement from Hurricane Andrew is not included in Table 1 because the anemometer system failed during the storm and it is not known whether the maximum wind speed was recorded. In Table 1, a negative percentage difference indicates that the maximum modeled wind speeds are lower than the maximum observed wind speeds.

Table 2 presents a summary of the percentage differences between simulated and measured wind speeds within a wind speed group. Fastest-mile wind speeds derived from either the peak gust or the mean wind-speed data are equally weighted. The results given in Table 2 indicate that the Shapiro-based wind-field model with a radial profile exponent,  $n$ , equal to 0.5 provides the best overall representation of the

hurricane wind-field. The Batts model clearly underestimates the maximum fastest mile wind speeds ( $V_{fm}$ ) near the eye wall ( $V_{fm} > 40$  m/s) and overestimates the lower wind-speed values away from the eye wall.

For inland stations, the Batts wind-field model overestimates the measured wind speeds. The mean and standard deviation of the ratio of observed to predicted fastest-mile wind speed obtained using the Batts wind-field model for the nine inland stations (Charlotte comparisons are not included) are 1.18 and 0.16, respectively. Using the Shapiro-based model (with  $n = 0.5$ ), the mean and standard deviation of the ratio of observed to predicted wind speeds are 1.03 and 0.09. The overestimation of wind speeds obtained using the Batts model is attributed to an underestimate or the reduction in the surface-level wind speed due to friction after the hurricane has moved inland. The minimum ratio of the surface-level wind speed to the upper-level wind speed in the Batts model is 0.73, which is notably higher than the value of 0.62 used in the implementation of the Shapiro-based model, or the value of 0.6 suggested by Powell (1987). At coastal land-based stations, positioned near the region of maximum winds, for Hurricanes Frederic, Alicia, and Elena, the Shapiro-based wind-field model performs better than the Batts wind-field model. The maximum wind speeds predicted by the Batts wind-field model at coastal locations, near the region of maximum winds, are generally lower than the measured values; the maximum wind speeds obtained from the Shapiro-based model agree well with the measured values, neither consistently overestimating or underestimating the peak wind speeds. The overall characteristics of the 12 to 24 h time series of wind speeds at these coastal locations are better modeled using the Sha-

TABLE 1. Percentage Difference between Peak Measured and Simulated Fastest-Mile Wind Speeds

Hurricane (1)	Measured Fastest-Mile Wind Speed (mi/hr)		Batts Model (%)		Shapiro-Based Model $n = 0.40$ (%)		Shapiro-Based Model $n = 0.50$ (%)		Shapiro-Based Model $n = 0.62$ (%)	
	A (2)	B (3)	A (4)	B (5)	A (6)	B (7)	A (8)	B (9)	A (10)	B (11)
Frederic										
Ingalls Shipyard	95	100	-5	-10	+13	+7	+13	+7	+12	+6
Mobile WSO	86	88	+9	+7	+9	+7	+8	+6	+5	+2
Pensacola Airport	68	70	+7	+4	+9	+6	-4	-7	-18	-20
Pensacola NAS	78	66	+3	+22	+6	+25	-3	+14	-16	-1
Elena										
Buoy 42007	65	—	+32	—	+2	—	-2	—	-6	—
Dauphin Island	102	107	-9	-14	+6	+1	+1	-5	+1	-5
Mobile WSO	50	52	+34	+28	+14	+8	+1	-3	-12	-17
Pensacola Airport	55	55	+13	+13	+11	+11	-4	-3	-18	-8
Pensacola NAS	68	64	+1	+6	+6	+11	-7	-3	-19	-16
Alicia										
Alvin	72	68	+12	+18	+9	+15	+9	+14	+8	+14
Buttonwood	85	104	+0	-17	+9	-10	+8	-11	+8	-11
Exxon Baytown	—	100	—	-18	—	-6	—	-6	—	-7
Dow "A"	70	77	+12	+1	+14	+6	+18	+7	+17	+9
WSO Galveston	85	80	+0	+5	-4	+1	-5	+0	-5	+0
Houston IAH	73	78	+9	+1	-5	-11	-7	-13	-7	-13
Ellington AFB	84	83	+2	+3	+4	+6	+3	+4	+2	+3
USCGC Clamp	—	84	—	+1	—	+1	—	-1	—	-3
Hugo										
Myrtle Beach AFB	71	78	-4	-5	+10	+9	+6	+5	-15	-16
Charleston NAS	112	94	-12	+6	+14	+37	+13	+36	+11	+33
Charleston Airport	85	82	+16	+21	+34	+39	+31	+37	+22	+27
Columbia Airport	60	62	+27	+21	+3	+0	+0	-5	-2	-6
Shaw AFB	104	95	-11	-2	-10	-3	-10	-3	-15	-7
Charlotte Airport	70	46	+31	+98	+30	+96	+27	+91	+24	+87
McEntire Airport	71	67	+17	+23	+6	+13	+7	+14	+6	+13
Florence	57	63	+52	+36	+27	+15	+18	+7	+6	-4
Andrew										
Molasses Reef	48	55	+73	+46	+24	+8	+5	-9	-18	-29

Note: A = derived from peak gust; B = derived from mean wind speed (1-, 2-, 10-, 15-, or 30-minute average).

**TABLE 2. Percentage Difference between Measured and Simulated Wind Speeds as Function of Wind-Speed Range**

Fastest-mile wind-speed range (mi/hr) (1)	Stations <sup>a</sup> (2)	Batts Model		Shapiro-Based Model $n = 0.40$		Shapiro-Based Model $n = 0.50$		Shapiro-Based Model $n = 0.62$	
		Mean (3)	SD (4)	Mean (5)	SD (6)	Mean (7)	SD (8)	Mean (9)	SD (10)
$V > 90^b$	1, 2, 3, 4, 16, 17	-8	7	5	14	4	14	2	14
$80 < V < 90$	5, 6, 18, 24, 25	7	8	12	15	10	14	8	10
$70 < V < 80$	7, 8, 9, 10, 19	6	7	8	5	6	9	-4	14
$60 < V < 70$	11, 12, 13, 20, 21, 22	21	16	9	8	2	9	-6	11
$V < 60$	14, 15, 23	25	14	13	6	-2	5	-19	6
All	All	12	23	11	17	6	17	0	19

Note: SD = standard deviation, WSO = Weather Service Office, NAS = Naval Air Station, and AFB = Air Force Base.

<sup>a</sup>1 = Ingalls Shipyard, 2 = Dauphin Island, 3 = USCGC Buttonwood, 4 = Exxon Baytown, 5 = Mobile WSO (Frederic), 6 = WSO Galveston, 7 = Pensacola NAS (Frederic), 8 = WSO Alvin, 9 = DOW Chemical Plant "A", 10 = Houston Intercontinental Airport, 11 = Pensacola Regional Airport, 12 = Data Buoy 42007, 13 = Pensacola NAS (Elena), 14 = Mobile WSO (Elena), 15 = Pensacola Airport (Elena), 16 = Charleston NAS, 17 = Shaw AFB, 18 = Charleston Airport, 19 = Myrtle Beach AFB, 20 = Columbia Airport, 21 = McEntire AFB, 22 = Florence, 23 = Molasses Reef C-MAN, 24 = Ellington AFB, and 25 = USCGC Clamp.

<sup>b</sup>Hurricane Andrew data not included because maximum wind speed was not recorded.

piro-based model. At near-coastal locations, away from the maximum winds, both models perform approximately equally well. At the overwater stations, wind speeds estimated using the Shapiro-based model agree well with the measured values, whereas the Batts wind-field model significantly overestimates the measured wind speeds when the overwater stations are on the left side of the storm (Buoy 42007 and Molasses Reef). This overestimate of the overwater wind speeds and slight underestimate of the near coastal wind speeds from the Batts model indicates that the sudden wind-speed reduction used in the Batts model is questionable. The good agreement for both the overwater and overland stations obtained using the Shapiro-based model indicates that the simple, gradual wind-speed decay is more realistic. Wind directions are modeled equally well using either wind-field models at or near the time the maximum wind speeds are measured.

Overall, the Shapiro-based wind-field model, with a radial profile exponent of 0.5, provides a good representation of the hurricane windfield. The two key points to note regarding the Batts wind-field model are the underestimation of the maximum winds near the eye wall, and the significant overestimation of wind speeds at inland stations. Neither of these deficiencies appear in the Shapiro-based wind-field model. It should be noted that all comparisons are for hurricanes making landfall in the southern portion of the United States. As described in Powell and Black (1990), in more northern regions, where the water temperature is lower than in the Gulf of Mexico and the South Florida Peninsula, the ratio of surface-level winds to upper-level winds is lower, suggesting that the surface-level, overwater wind speeds may be overestimated using either of the wind-field models described here for the North Atlantic Coast.

## FILLING-RATE MODELS

Once a tropical cyclone makes landfall it weakens as the central pressure rises. This rate of weakening varies with storm, location of landfall, and the central pressure difference at the time of landfall ( $\Delta p_0$ ). Proper modeling of the filling of the storms is important for the prediction of hurricane winds at inland locations. Schwerdt et al. (1979) studied 16 landfalling hurricanes and subdivided the filling rates into three different geographic regions (Gulf Coast, Florida peninsula, and Atlantic Coast). They found that hurricanes making landfall on the Florida peninsula filled the slowest and storms making landfall on the Gulf Coast filled fastest. Ho et al. (1987) used the same three geographic regions used by Schwerdt et al. (1979) to define the filling rates. Along the Gulf Coast and the Florida peninsula they represent three filling-rate curves

[for storms with values of  $\Delta p_0$  of 110, 100, and 85 millibar (mbar), with the more intense storms filling more rapidly than the weak ones]. Along the Atlantic Coast they present only one filling-rate curve.

Georgiou (1985) developed filling models for four geographic regions (western Gulf Coast, central Gulf Coast, Florida Peninsula, and the Atlantic Coast). He departed from the commonly used models, where filling is dependent on the time since landfall, and developed models based on the distance traveled since making landfall, with no dependence of the storm filling rate as a function of intensity.

The filling-rate model used by Batts et al. (1980) is independent of location and intensity at landfall. The filling rate used by Batts et al. (1980) is given as

$$\Delta p(t) = \Delta p_0 - 0.675(1 + \sin \phi)t \quad (13)$$

where  $\Delta p(t)$  = central pressure difference (mbar) at  $t$  h after landfall; and  $\phi$  = angle between the storm direction and the coastline at the point of landfall.

In this study, three different filling-rate models were developed using central pressure and position data given in HURDAT. For storms making landfall on the Gulf Coast, 20 storms were used. Nine storms were used to develop filling-rate models in each of the Atlantic Coast and Florida Peninsula regions. The filling rates were modeled in the following form:

$$\Delta p(t) = \Delta p_0 \exp(-at) \quad (14)$$

The filling constant  $a$  is given as

$$a = a_0 + a_1 \Delta p_0 + \varepsilon \quad (15)$$

where  $\varepsilon$  = a normally distributed error term with a mean of zero. The constants  $a_0$  and  $a_1$  and the standard deviation of the error term,  $\sigma_\varepsilon$ , for each of the three geographic regions are given in Table 3. Fig. 3 shows the fitted values of the decay constant,  $a$ , plotted versus the central pressure difference at the time of landfall for each of the three geographic regions. In the case of the Gulf Coast storms, the exponential decay model was found to reproduce observed filling rates better when a 2-h delay was incorporated into the model.

**TABLE 3. Exponential Filling-Rate Constants**

Region (1)	$a_0$ (2)	$a_1$ (3)	$\sigma_\varepsilon$ (4)	$r^2$ (5)
Florida Peninsula	0.006	0.00046	0.0025	0.8
Gulf Coast	0.035	0.00050	0.0355	0.07
Atlantic Coast	0.038	0.00029	0.0093	0.16



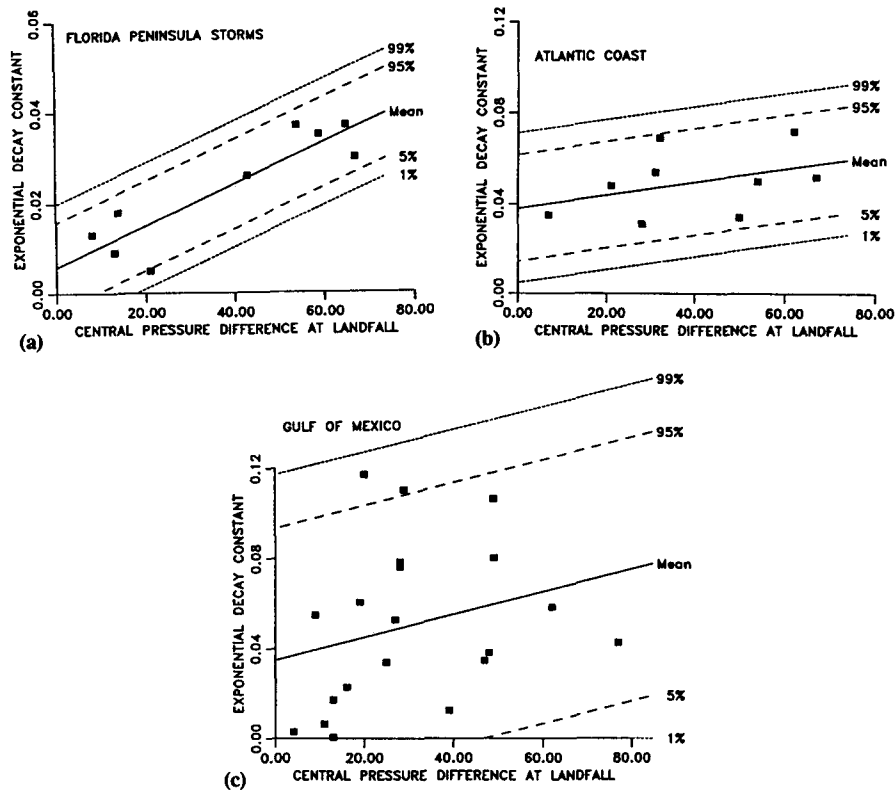


FIG. 3. Filling Constant  $a$  versus Central Pressure Difference at Landfall

The filling-rate models developed here and the filling-rate model used by Batts et al. (1980) were evaluated through comparisons of detailed filling studies presented in Ho et al. (1987). Tables 4–6 show the mean and standard deviation of the difference (in mbar) between the predicted and observed increase in central pressure with time after landfall for the three regions. All of the hurricanes used in the comparison

TABLE 4. Difference between Modeled and Observed Increase in Central Pressure (mbar) after Landfall Using New and Batts Filling Models for Gulf Coast

Filling-rate model	Time after landfall (h)						Unweighted composite average
	2	4	6	8	10	12	
New filling model							
Mean (mbar)	6.3	3.8	2.5	0.9	2.6	3.2	3.2
SD (mbar)	8.7	11.5	11.7	11.3	10.6	8.8	10.4
Batts filling model							
Mean (mbar)	4.3	7.1	10.3	14.4	17.9	20.5	12.4
SD (mbar)	8.6	13.7	15.6	17.4	16.4	16.2	14.4

Note: SD = standard deviation.

TABLE 5. Difference between Modeled and Observed Increase in Central Pressure (mbar) after Landfall Using New and Batts Filling Models for Florida Peninsula

Filling-rate model	Time after landfall (h)			Unweighted composite average
	3	6	9	
New filling model				
Mean (mbar)	2.9	−2.3	−4.3	−1.2
SD (mbar)	9.2	3.9	4.4	5.8
Batts filling model				
Mean (mbar)	7.4	3.3	2.8	4.5
SD (mbar)	11.2	3.8	2.8	5.9

Note: SD = standard deviation.

TABLE 6. Difference between Modeled and Observed Increase in Central Pressure (mbar) after Landfall Using New and Batts Filling Models for Atlantic Coast

Filling-rate model	Time after landfall (h)						Unweighted composite average
	2	4	6	8	10	12	
New filling model							
Mean (mbar)	−0.9	−0.1	0.1	0.4	2.6	−0.8	0.2
SD (mbar)	1.6	2.7	4	5.1	3.7	2.7	3.3
Batts filling model							
Mean (mbar)	2.5	7.9	8.3	10.2	14.2	9.6	8.8
SD (mbar)	1.9	4.8	6.9	9	11.2	9.6	7.2

Note: SD = standard deviation.

had central pressure differences at landfall of 25 mbar or more. A positive difference indicates that the modeled results are conservative. The data given in Tables 4–6 indicate that the new filling model is slightly conservative for Gulf Coast storms, slightly nonconservative for Florida storms, and approximately mean-centered for Atlantic Coast storms. The filling-rate model used by Batts et al. (1980) is conservative in all regions, and on average this conservatism increases with time after landfall.

The filling-rate models developed here reproduce the observation that intense storms fill more rapidly than weak storms, as noted in Tuleya et al. (1984) in their investigation examining both historical storms and simulated storms. The introduction of a random error term allows for the simulation of storms that fill much more slowly or rapidly than average.

## EFFECT OF COMBINED WIND-FIELD AND FILLING MODELS ON WIND SPEEDS AT INLAND LOCATIONS

To examine the combined effect of the filling models and wind-field models on wind-speed estimates, simulations of hurricane wind speeds at 9 of the 10 inland stations examined

**TABLE 7. Comparison of Simulated and Observed Wind Speeds at Inland Locations Showing Combined Effect of Filling Models and Windfield Models**

Hurricane (1)	Location (2)	Distance inland (km) (3)	Simulated fastest-mile wind speed divided by observed fastest-mile wind speed (Shapiro-based wind-field and new filling model) <sup>a</sup>		Simulated fastest-mile wind speed divided by observed fastest-mile wind speed (Batts wind-field and Batts filling models) <sup>b</sup>	
			A (4)	B (5)	A (6)	B (7)
Frederic	Mobile	17 <sup>c</sup>	1.09	1.06	1.18	1.15
Alicia	Alvin	30	1.09	1.14	1.13	1.19
Alicia	Houston (IAH)	50 <sup>d</sup>	0.88	0.82	1.14	1.07
Alicia	USCGC Clamp	20 <sup>d</sup>				1
Hugo	Columbia	180	1.13	1.1	1.58	1.53
Hugo	Shaw AFB	130	0.91	1	1.07	1.17
Hugo	McEntire AFB	140	1.1	1.16	1.44	1.52
Hugo	Florence	100	1.14	1.03	1.75	1.59
Hugo	Charlotte	290	1.33	2.02	1.6	2.43

Note: A = based on peak gust; B = based on mean wind speed; and SD = standard deviation.

<sup>a</sup>With Charlotte measurement, mean = 1.12 and SD = 0.26; without Charlotte measurement, mean = 1.04 and SD = 0.1.

<sup>b</sup>With Charlotte measurement, mean = 1.38 and SD = 0.36; without Charlotte measurement, mean = 1.3 and SD = 0.24.

<sup>c</sup>Distance from Mobile Bay.

<sup>d</sup>Distance from Galveston Bay.

earlier were performed. The Mobile, Ala., wind speeds recorded during Hurricane Elena are not included in this comparison because the maximum wind speeds were observed before the hurricane made landfall. In these storm-specific simulations, the central pressure difference at landfall is used to initiate the simulation and is then decreased once landfall is made using the filling models described earlier. This simulation approach reproduces wind speeds at inland locations similar to those that would be obtained in an actual simulation. The results of the simulations are given in Table 7, where it is clearly seen that the combination of the Batts filling model and Batts wind-field model yield conservative estimates of wind speeds at inland locations, with a mean overestimate of 38%. The overestimate of wind speeds produced by the Batts models increases with distance from the coast. The combination of the Shapiro-based wind-field model and new filling models, though still yielding conservative results, overestimates the observed wind speeds by only 12%. When the anomalous Charlotte wind-speed measurement is removed from the comparisons, the mean overestimate of the observed wind speeds obtained using the Shapiro-based wind-field model and the filling models is 4%, whereas if the Batts models are used the overestimate is 30%.

## SUMMARY AND CONCLUSIONS

Extensive evaluation of the wind-field models clearly indicates that the model used by Batts et al. (1980) underestimates the maximum wind speeds in intense hurricanes near the eye wall at coastal locations, and overestimates wind speeds at inland locations. These deficiencies are not evident in the Shapiro-based wind-field model. The evaluation of the filling models indicates that the model used in Batts et al. (1980) is conservative, and the combined deficiencies in the Batts filling model and wind-field model result in a significant overestimate of wind speeds for inland locations. The Shapiro-based wind-field model combined with the new filling models are believed to provide better predictions of hurricane wind speeds at both near-coastal locations and inland locations than do the results of earlier studies; however, further research into the rate of reduction of wind speeds near the surface after a hurricane makes landfall is required. Further comparisons between modeled and observed wind speeds for storms making landfall in the northern United States are also required to improve the reliability of the model to estimate

wind speeds in fast moving hurricanes traveling over cold water.

## APPENDIX. REFERENCES

- Amoroch, J., and Devries, J. J. (1980). "A new evaluation of wind stress coefficient over water surfaces." *J. Geophys. Res.*, 85, 433-442.
- Batts, M. E., Cordes, M. R., Russell, C. R., Shaver, J. R., and Simiu, E. (1980). "Hurricane wind speeds in the United States." *Nat. Bureau of Standards Rep. No. BSS-124*, U.S. Dept. of Commerce, Washington, D.C.
- Chow, S. H. (1971). "A study of windfield in the planetary boundary layer of a moving tropical cyclone," MS thesis in Meteorology, School of Engrg. and Sci., New York Univ., New York, N.Y.
- Donelan, M. A. (1982). "The dependence of the aerodynamic drag coefficient on wave parameters." *Proc., 1st Int. Conf. on Meteorology and Air/Sea Interaction of the Coast. Zone*, 351-367.
- Durst, C. (1960). "Wind speeds over short periods of time." *The Meteorological Mag.*, 89(1056), 181-187.
- Georgiou, P. N. (1985). "Design wind speeds in tropical cyclone-prone regions," PhD thesis, Fac. of Engrg. Sci., Univ. of Western Ontario, London, Ont., Canada.
- Golden, J. H. (1984). "Meteorological overview of Hurricane Alicia." *Proc., Spec. Conf., Hurricane Alicia: One Year Later*, ASCE, New York, N.Y., 1-20.
- Ho, F. P., et al. (1987). "Hurricane climatology for the Atlantic and Gulf Coasts of the United States." *NOAA Tech. Rep. NWS38*, Federal Emergency Mgmt. Agency, Nat. Oceanic and Atmospheric Admin. (NOAA), Washington, D.C.
- Kaplan, J., and Frank, W. M. (1993). "The large-scale, inflow-layer structure of Hurricane Frederic (1979)." *Monthly Weather Rev.*, 121(1), 3-20.
- Krayer, W. R., and Marshall, R. D. (1992). "Gust factors applied to hurricane winds." *Bull. Am. Meteorological Soc.*, 73(5), 613-617.
- Marshall, R. D. (1984). "Fastest-mile wind speeds in Hurricane Alicia." *Nat. Bureau of Standards Tech. Note No. 1197*, U.S. Dept. of Commerce, Washington, D.C.
- "Minimum design loads for buildings and other structures." (1990). ASCE-7-88, ASCE, New York, N.Y.
- Myers, V. A. (1954). "Characteristics of United States hurricanes pertinent to levee design for Lake Okeechobee, Florida." *Hydrometeorological Rep. No. 32*, U.S. Dept. of Commerce, Washington, D.C.
- Powell, M. D. (1980). "Evaluations of diagnostic marine boundary-layer models applied to hurricanes." *Monthly Weather Rev.*, 108, 757-766.
- Powell, M. D. (1982). "The transition of Hurricane Frederic (1979), boundary-layer wind field from the open Gulf of Mexico to landfall." *Monthly Weather Rev.*, 110, 1912-1932.
- Powell, M. D. (1987). "Changes in the low-level kinematic and thermodynamic structure of Hurricane Alicia (1983) of landfall." *Monthly Weather Rev.*, 115(1), 75-99.
- Powell, M. D., and Black, P. G. (1990). "The relationship of hurricane reconnaissance flight-level wind measurements to winds measured by

- NOAA's oceanic platforms." *J. Wind Engrg. and Industrial Aerodynamics*, 36, 381–392.
- Powell, M. D., Dodge, P. P., and Black, M. L. (1991). "The landfall of Hurricane Hugo in the Carolinas: surface wind distribution." *Weather and Forecasting*, 6, 379–399.
- Powell, M. D., and Houston, S. (1993). "Surface wind field analyses in Hurricane Andrew." *Proc., 20th Conf. on Hurricanes and Tropical Meteorology*, Am. Meteorological Soc., Boston, Mass.
- Roll, H. U. (1965). *Physics of the marine atmosphere*. Academic Press, New York, N.Y.
- Schwerdt, R. W., Ho, F. P., and Watkins, R. R. (1979). "Meteorological criteria for standard project hurricane and probable maximum hurricane windfields, Gulf and Atlantic Coasts of the United States." *NOAA Tech. Rep. NWS23*, U.S. Dept. of Commerce, Washington, D.C.
- Shapiro, L. J. (1983). "The asymmetric boundary layer flow under a translating hurricane." *J. Atmospheric Sci., AMS*, 40(8), 1984–1998.
- Tuleya, R. E., Bender, M. A., and Kurihara, Y. (1984). "A simulation study of the landfall of tropical cyclones using a moveable-mesh model." *Monthly Weather Rev.*, 112(1), 124–136.
- Twisdale, L. A., and Vickery, P. J. (1992). "Predictive methods for hurricane winds in the United States." *Final Rep., Small Business Innovation Res. Grant ISI916035*, Nat. Sci. Found., Washington, D.C.
- Willoughby, H. E. (1990). "Temporal changes of the primary circulation in tropical cyclones." *J. Atmospheric Sci.*, 47(2), 242–264.